ROCK WEATHERING ALONG SMALL MOUNTAINOUS RIVERS: SIERRA DE LAS MINAS, GUATEMALA

Research Thesis

Submitted in partial fulfillment of the requirements for graduation

with research distinction in Earth Sciences in the undergraduate colleges of

The Ohio State University

By

Laura A. Miller

The Ohio State University

2016

Approved by

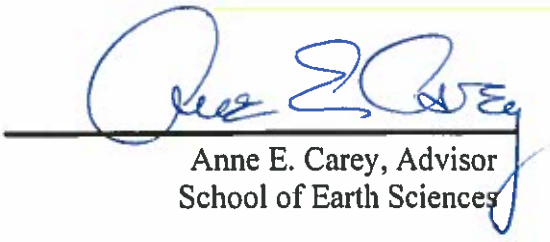

Anne E. Carey, Advisor
School of Earth Sciences

TABLE OF CONTENTS

Abstract……...iii

Acknowledgements…….……iv

List of Figures……..v

List of Tables……..….v

Introduction……..1

Geologic Setting

Regional tectonics…….…….……..…..…..2

Lithology……..2

Climate and Hydrology……..……..…..…….3

Methods

Field Area…...…….…….5

Sampling Methodology…….…….……..5

Light Microscopy……...…..……....6

XRF Major Oxide Analysis…...……..……....…...6

Scanning Electron Microscope and Elemental Spot Analysis……...…..7

XRD Analysis……...…….…..7

Results

Petrology……..8

Concentrations of Major Elements……...……...……9

Mineralogy……...……...…11

Rare Earth Bearing Mineral Phases…...……...…….14

Discussion

Weathering of the Rock Interior……15

Origins of minerals……..……. …….……..15

Calcium Contributors……...…….15

Implications of epidote-group weathering……...…..15

Ferrolysis and Carbonate Dissolution……...…….16

Conclusions……17

Suggestions for Future Research……...……18

References Cited….…….……..19

Appendices

Appendix A……21

Bead Making Method

Appendix B……22

Corrected Major Oxide Concentrations

Appendix C……23

XRD Results

Abstract

Studies of chemical weathering in small mountainous rivers have shown their disproportional role in chemical weathering and delivery of dissolved and particulate materials on a global scale. Previous stream water analyses from La Sierra de Las Minas have shown higher than expected Ca/Na ratios in all streams studied. While the stream chemistry is known, it is important to understand the mineralogy, petrology, and lithology of the area to gain insight into the origins of these chemical weathering products. SEM imaging and elemental mapping of stream cobble samples have shown the presence of calcium bearing minerals such as albite, epidote, apatite, garnet, carbonates and allanite. Mineral grains exhibited dissolution textures across a range of samples, mainly consisting of meta-granites, gneisses, and schists. Analyses of these rocks using x-ray fluorescence analysis was used to determine the major oxide content of the stream cobbles. When normalized to upper continental crust all rock samples show a depletion in calcium with the exception of one sample containing calcium carbonate. While the samples were depleted in the majority of major oxides, silica content was similar to that of upper continental crust. A variety of samples show preferential weathering of calcium bearing mineral phases both under microscope and in XRF major oxide analysis results. This suggests stream bed cobbles are not sources of minerals for silica weathering, but do impact the input of calcium into the streams.

ACKNOWLEDGEMENTS

I would like to extend my thanks to everyone who has supported me in my undergraduate career. First and foremost, I would like to thank my family for their ongoing support and encouragement. Without them I would not be the person I am today, nor would I have had the incredible opportunities that have lead me to where I am, and where I am headed. I would also like to thank my friends for being there when labs were long and sleep was in short supply. Earth science would not be the same without all of the amazing people I have met along the way. Very importantly I would like to thank the Ohio State School of Earth Sciences faculty and staff. In particular I would like to show my appreciation for Dr. Anne Carey, my advisor and mentor from the start of my college career, Dr. Sue Welch, my advisor and microscopy companion, as well as, Dr. Julie Sheets, Brandon McAdams, and Dan Audrey for all their help in my research. Finally, I would like to thank the Shell Exploration and Production Company for a wonderful summer of 2015 research opportunity and funding, along with Friends of Orton Hall for providing funding for my trip to GSA Annual Meeting 2015 in Baltimore to present my research and the NSF grants that aided in the collection and analysis of my samples, NSF DEB 0919138, NSF GEO EAR SGER 0909271, NSF DEB 0919043 and NSF EAR Instrumentation and Facilities 0135318.

List of Figures

1. General geology
2. Rivers on the north side of La Sierra de las Minas
3. Sierra de las Minas watershed and elevations
4. Field area
5. Sampling locations
6. Major oxide concentrations normalized to upper continental crust
7. Elemental differences within epidote grains
8. Fe-Mg rich carbonate within the interior
9. Carbonate dissolution along the exterior
10. Garnet dissolution and fracturing
11. Apatite weathering on weathering rind
12. Clay weathering
13. Allanite weathering

List of Tables

1. Sampling locations
2. Rock sample descriptions

Introduction

Since the pioneering work of Milliman and Syvitski (1992), small mountainous rivers have been the subject of study as important contributors of particular weathering products to the world ocean. More recently, attention has turned to these same small mountains rivers as conduits of dissolved weathering products to the ocean (Goldsmith et al., 2015; Jacobson and Blum, 2003; Lyons et al., 2005; McAdams et al., 2015). Geographically, most of these systems are around the Pacific Rim including regions of Taiwan, New Zealand and Guatemala.

La Sierra de las Minas, like other small mountainous river systems, has a disproportionately large weathering flux according to stream water chemistry. Analysis of water samples showed a Ca/Na ratio greater than expected based on plagioclase weathering or bulk rock composition (McAdams , 2012; McAdams et al., 2015). The molar Ca/Na ratios ranged from 0.29–2.5 across rivers on the north side of the range (McAdams , 2012). If plagioclase weathering cannot explain the observed Ca/Na molar ratios in the stream water chemistry, this poses the question "what is weathering is La Sierra de Las Minas?"

Small mountainous river systems have exhibited a trend of higher than once predicted contributions to the global weathering budget (Carey etal., 2005; Goldsmith , 2005; Jacobson and Blum, 2003; Lyons et al., 2005; Milliman and Syvitski, 1992). It is likely that these higher than expected weathering rates are a result of physical weathering coupled with high chemical weathering rates. The consistent replenishment of fresh weathering surfaces due to physical processes creates more opportunity for chemical weathering to occur. Furthermore, streambed rocks are likely to have an impact on solute input within small mountainous river systems. For that reason, streambed rocks should be taken into account when predicting weathering flux in these systems.

The phrase "calcium problem" has been used to explain the higher than expected Ca/Na ratios in spring water when predicted by the dissolution of plagioclase (Bowser and Jones, 2002). It was found that the "calcium problem" was not specific to one type of environment, but existed for spring waters, subalpine watersheds, and mountainous rivers among others. It was stated that mineralogy is a notable control of Ca/Na rations in steam water chemistry (Bowser and Jones, 2002). Therefore, local mineralogy must be understood in order to properly predict the input of calcium into surface waters.

This study focused on the possible origins of the weathering products observed in the water chemistry. In order to do so, the mineralogy and petrology of stream cobbles will be taken into account along with the regional lithology. By gaining an understanding of the extent of weathering of particular minerals, the importance of these minerals to the weathering flux can be determined.

GEOLOGIC SETTING

Regional Tectonics

La Sierra de las Minas mountain range is framed by fault controlled river valleys that are a result of sinistral strike-slip faults (Marshall, 2007). There is evidence that suggests the Polochic fault, where the Polochic river valley lies, was once the primary plate boundary between the North American and Caribbean plates. The Polochic fault is on the north side of La Sierra de las Minas, trending east to west, with the Motagua fault mirroring the Polochic on the south side of the mountain range (Figure 1). The rivers flowing along these faults are named accordingly and are fed by the rivers and tributaries which are the focus of this study.

Due to regional uplift events in the Late Miocene and Quaternary, there has been noticeable stream reorganization in the rock record. The west to east trending uplift of the Sierra de las Minas was the cause for the diversion of the Chixóy River. Today the Chixóy is one of the largest rivers in La Sierra de las Minas and possibly one of the greatest contributors of calcium into the system due to an underlying gypsum bed (Brocard et al., 2011).

Lithology

La Sierra de las Minas is mainly composed of Late Paleozoic to Cretaceous metamorphic rocks including felsic gneiss, marble, quartzite, schist, and eclogite (Bundschuh, 2007). These rocks are a result of the regional tectonics surrounding the Maya block where Sierra de las Minas is situated. Some formation are well characterized but still the region lacks adequate detailed mapping, although generalized maps have been produced in the past (Figure 1).

The Jones Formation is the main constituent of La Sierra de las Minas. This formation consists of politic schists, phyllites, marble and minor amounts of quartzite (large marble outcrops were observed during sample collection). In addition, green actinolite interbedded within the Jones Formation (Bundschuh, 2007). Within the Jones Formation lies the San Lorenzo Formation or the San Lorenzo marble. It can be seen in large outcrops in the central and eastern parts of La Sierra de las Minas. Today it is debated as to whether or not the San Lorenzo marble and the Jones Formation should be separated into two units or remain as one (Bundschuh, 2007).

Along the Motagua suture zone there are ophiolites which are primarily composed of serpentinite and brecciated peridotite. These rock units, also seen in orogenies adjacent to the Motagua fault, like La Sierra de las Minas, are referred to as the El Tambor group. A characteristic of the El Tambor group is that metamorphosed volcanic rocks that have been replaced and now host minerals such as chlorite, calcite, albite, and pumpellyite (Bundschuh, 2007).

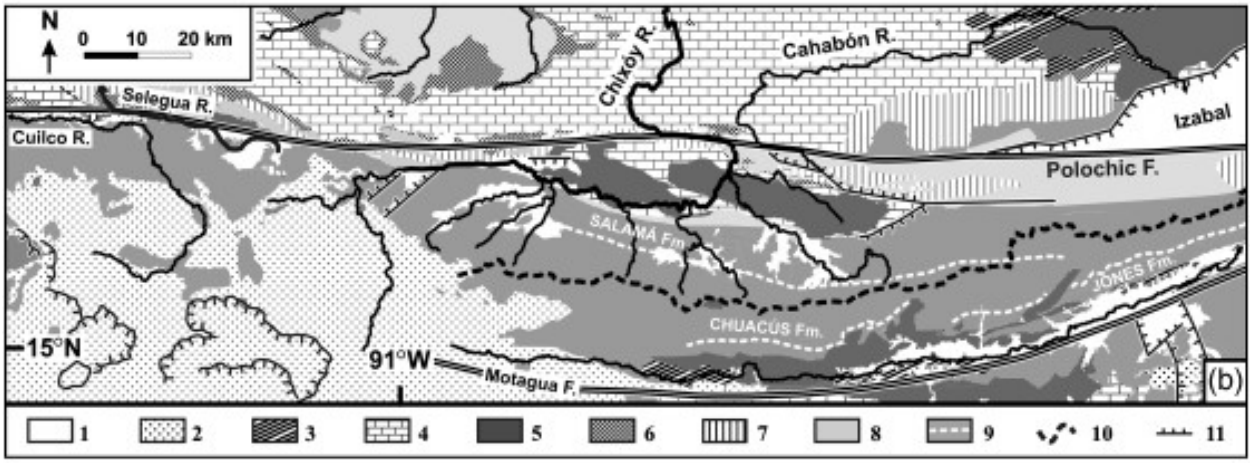

Figure 1: General geologic map of La Sierra de Las Minas. 1) Quaternary; 2) Neogene-Quaternary volcanics; 3) Late Cretaceous-Oligocene terrigeneous sediments; 4) Cretaceous limestone; 5) Ophiolites; 6) Upper Jurassic terrigenous; 7) Permian limestones; 8) Permian siliciclastics; 9) Basement with boundaries between main formations; 10) SCSM draninage divide; 11) Normal fault (Brocard et al., 2011).

Climate and Hydrology

The north side of La Sierra de las Minas receives significantly more rainfall than the south side of the range due to the rain shadow created by the roughly 3000m elevation of the range (McAdams et al., 2015). Stream morphology in the area was strongly influenced by tectonic activity between the Late Miocene and the Quaternary. Pathways were controlled primarily by limestone belts and fault zones (Brocard et al., 2011). An example of fault controlled drainage are the Polochic and Montagua rivers which frame the mountain range along their respective faults. The watershed of la Sierra de las Minas lies south (Figure 3) of the rivers running down the north side of the mountain (Figure 2).

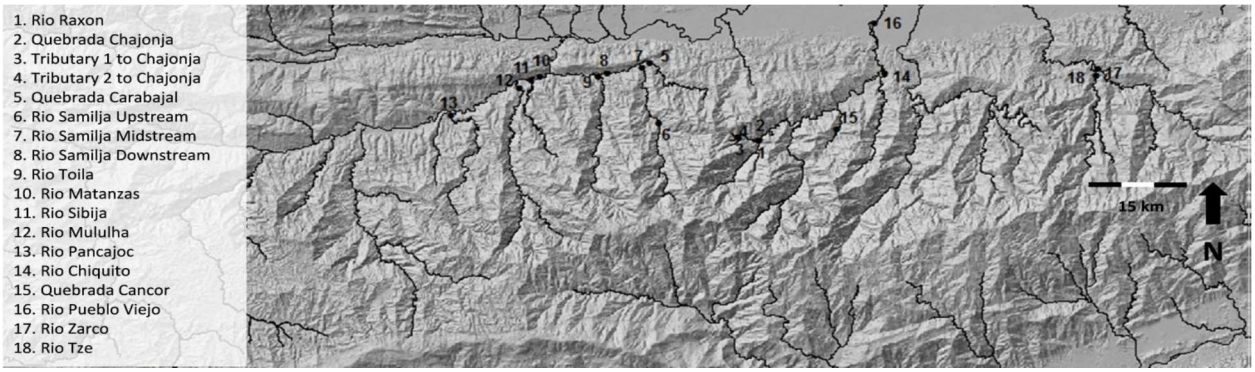

Figure 2: Rivers on the north side of La Sierra de las Minas (McAdams , 2012).

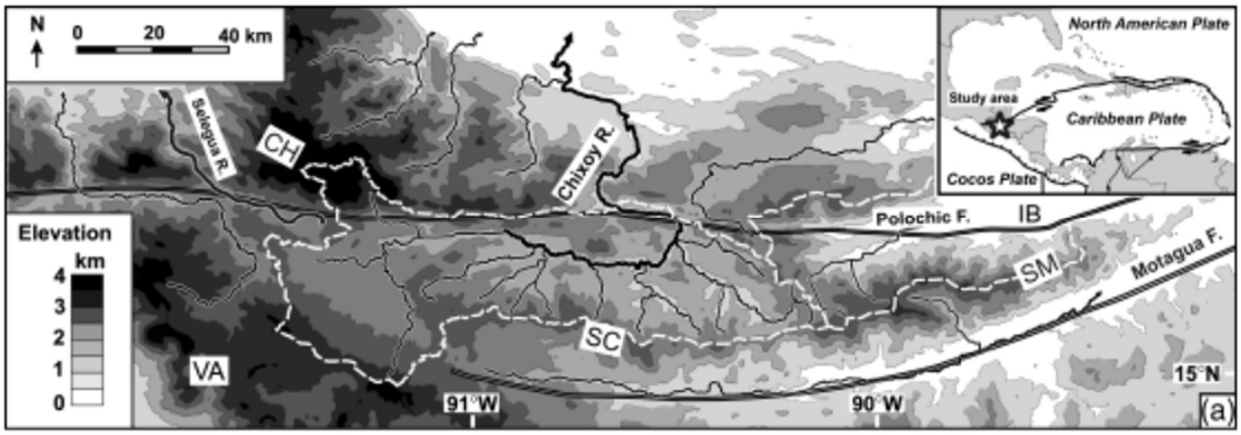

Figure 3: Outline of the watershed identified by the white dashed line (figured from Brocard et al., 2011).

METHODS

Field Area

The area of study is located in eastern Guatemala on the north side of Sierra de las Minas (Figure 4). Sierra de las Minas is a mountain range reaching elevations of roughly 3000 meters with mean annual rainfall throughout the year of 2400–2600 mm yr^{-1} on the north side (McAdams et al., 2015). The mountain range hosts of multiple rivers and tributaries from which sediment, water, and stream cobble samples were collected.

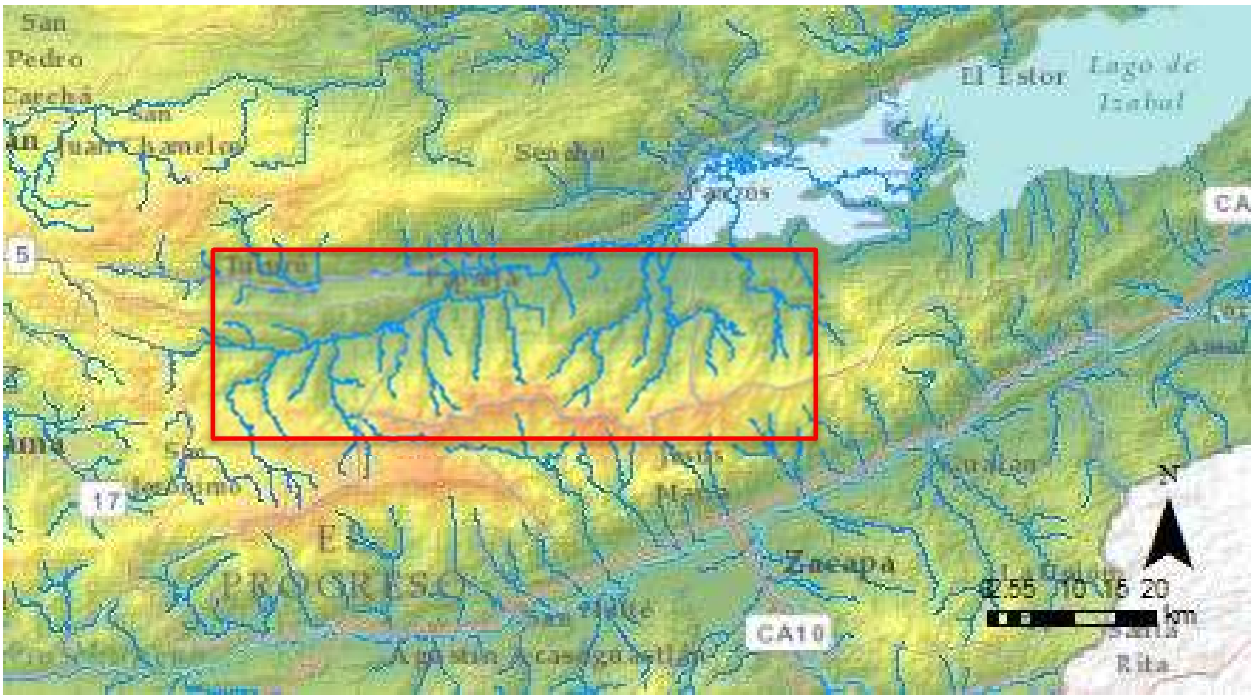

Figure 4: The north side of Sierra de las Minas outlined by the red box.

Sampling Methodology

Between February and March of 2012 collection of sediment, water, and stream cobble samples took place at various location along the north side of the mountain range (McAdams, 2012). Stream cobbles were collected along the edge of streams and correspond to water and sediment samples from each respective location. In total, eight samples were collected and later analyzed from eight rivers (Table 1, Figure 5).

Table 1: Modified from McAdams et al., 2015. UTM coordinates used based on the North American Datum 1983, section 16P. Some sample locations included multiple samples such as 08A and 08B.

Sample Number	River Name	Latitude	Longitude	Elevation (m)
01	Río Raxon	203793	1685324	582
02	Quebrada Chajonja	230705	1685359	909
04	Río Samilija	196673	1686851	516
08	Río Mululha	186861	1689833	184
07	Río Sibija	187709	1690469	162
10	Tributary 1 to Chajonja	202349	1685564	810
12	Río Toila	192453	1690654	231
18	Río Zarco	227914	1690729	185

Figure 5: Sampling locations labeled using Google

Light Microscopy

After an examination of all available hand samples, a representative group of rock samples, from eight different rivers including some granitic in composition, metamorphic, and an unknown sample were chosen to be cut into thin section. In all, seven samples were sent to Spectrum Petrographics to be cut into thin sections. Each sample was impregnated with epoxy and died blue then cut to 30μm thick.

Light microscopy was used for an initial determination of the mineral constituents of each rock samples. The thin sections were observed in polarized, cross-polarized, and reflective light. These results then served as reference point for the subsequent SEM analysis.

XRF Major Oxide Analysis

Samples were crushed into a fine powder using a SPEX CertiPrep 8515 Shatterbox then dried for a minimum of 12 hours at 110 ˚C. The powder was then combined with lithium tetraborate in a 1:4 ratio and melted in a platinum crucible at roughly 1220˚C using a Philips Perl'x 3. The melt

was then cast in a platinum dish and labeled accordingly. Please refer to Appendix A for more detailed glass bead making methods.

Each sample was analyzed in a Panalytic XRF MagiX PRO x-ray fluorescence spectrometer with an analysis repeat count of 3 and at least one standard analyzed as an unknown to gauge the accurateness of the data. Each sample took roughly three hours to complete one full analysis. When not being analyzed, glass beads were stored in plastic cases in a desiccator to prevent water from entering the sample.

Scanning Electron Microscope and Elemental Spot Analysis

Both thin sections and small pieces of rock were placed on stubs for analysis with an FEI Quanta FEG 250 SEM. Before being placed in the SEM, all samples were coated using a Denton Desk V precious metal coater, in a mixture of gold and palladium to prevent the surface from becoming charged. Carbon tape was used to secure the samples on the stubs.

Both types of samples had benefits and drawbacks. The advantage to using thin sections was the ability to retrieve accurate mineral mapping of the thin section surface. The disadvantage of using thin sections was the lack of a natural weathered surface to get an image of weathering textures. On the other hand, small pieces of the rock, both of the rock's interior and the weathered exterior, provided images of the naturally weathered surface. The major disadvantage is that due to the pits in the small bits of rock it was not always possible to determine elemental composition due to the distance from the electron detector.

Qualitative analysis of the mineralogy was conducted using back scatter electron microscopy and Bruker energy dispersive X-ray spectrometer (EDS). Secondary electron detector images were also taken in order to observe mineral surfaces. In some cases, elemental spot analysis was also used in order to determine possible mineralogy and elemental differences within individual grains.

XRD Analysis

Dried, powdered, samples were loaded into a PANalytical X'Pert Pro using a two theta angle of 5-70. Software helped to detect possible minerals present in each sample, but required editing prior to interpretation. There was minimal background interference and the peaks were relatively clean, but some peaks detected need to be removed and some peaks need to be added manually (Appendix C). Once the data are treated, minerals can be identified using a comprehensive mineral database.

RESULTS

Petrology

The majority of samples were analyzed in thin section and SEM, but some samples were only analyzed using XRF analysis (Table 2). The majority of samples were igneous in origin and mostly metamorphosed to some extent. The samples were all felsic in nature with the exception of sample 08B which could not be identified, but does include carbonate.

Table 2. Rock identification in hand sample, mineralogy by petrographic microscope and mineralogy by SEM inspection and spot analysis.

Sample	Rock Type	Petrographic Microscope	SEM
01A	Granitic Gneiss	Consists of quartz, feldspar with tartan twinning, hornblende. Myrmekitc-like textures seen throughout the sample, but consisted of epidote and albite. Observed a clear in PPL fibrous mineral, most likely rutile.	Mainly composted of potassium feldspar, biotite, muscovite and feldspar (oligoclase-albite in composition). Veins filled with a titanium-rich mineral, likely ilmenite. Observed zircons with apatite inclusions and thorium-rich monazites. Crystallographic controls on weathering of feldspar observed.
02	Gneiss (XRF Only)	N/A	N/A
04C	Heavily Weathered Granite	N/A	Contained small amounts of heavily weathered monazite throughout. Inclusions of lead sulfide seen in apatite grains.
08A	Diorite	Contains biotite with pleochroic halos, quartz and some muscovite. Felty texture with 2nd and 3rd order colors in XPL, but grains were too small to identify.	Secondary minerals included apatite and pyrite. Biotite mica seen in a groundmass of albite. Albite showed signs of weathering, including dissolution pits. Weathered surface was covered in biogenic material and mineral precipitates. Apatite grains also covered in biogenic material and surrounded by muscovite mica. Epidote throughout sample as needle-like crystals surrounded by albite.
08B	Unknown	Carbonate seen in interior and in decreasing amounts moving towards the exterior. Felty grains with high birefringence observed, but too small to accurately identify.	Mostly albite and carbonate with Mg and Fe. Carbonate is surrounded by iron oxy hydroxides. Fractures and pore spaces increase towards the exterior of the sample.

103	Meta-Diorite	Large quartz and feldspar phenocryst with tartan twining and some Carlsbad twinning. Sillimanite in veins and abundant along the weathering rind. Quartz is also vein fill. In some area crushed quartz grains are mixed with this fibrous mineral.	N/A
12	Meta-Schist	Small, needlelike epidote with weak yellow to green pleochroism and up to 3rd order colors in XPL. Iron banding seen throughout the sample along foliation and within some fractures. Grains appear to be foliated within themselves and decrease in size moving from the interior to the exterior. Rock consists mainly of quartz with very little plagioclase.	Large amounts of graphite or organic material as well as quartz and albite. Small grains of chlorite seen between platy graphite grains. Xenotime and monozites seen on the surface and within the interior of the sample. Also, saw clays and biofilm on the weathered surface, but unable to get an accurate signal from the BSED. Outlines of what appears to framboidal pyrite filled by iron. Saw small flecks of bismuth in the sample.

Concentration of Major Elements

Major oxide percentages were corrected to 100% total concentration (Appendix A) then normalized to bulk major oxide composition of upper continental crust (Figure 6) using data from Rudnick and Gao (2003). A total of eight representative samples were analyzed. Sample compositions ranged from mostly granitic in nature to stream cobbles rich in clay minerals. All samples have similar SiO_2 and Na_2O compositions relative to upper continental crust. The majority of samples with the exception of 08B, which contains carbonate, show a depletion in calcium when normalized to continental crust.

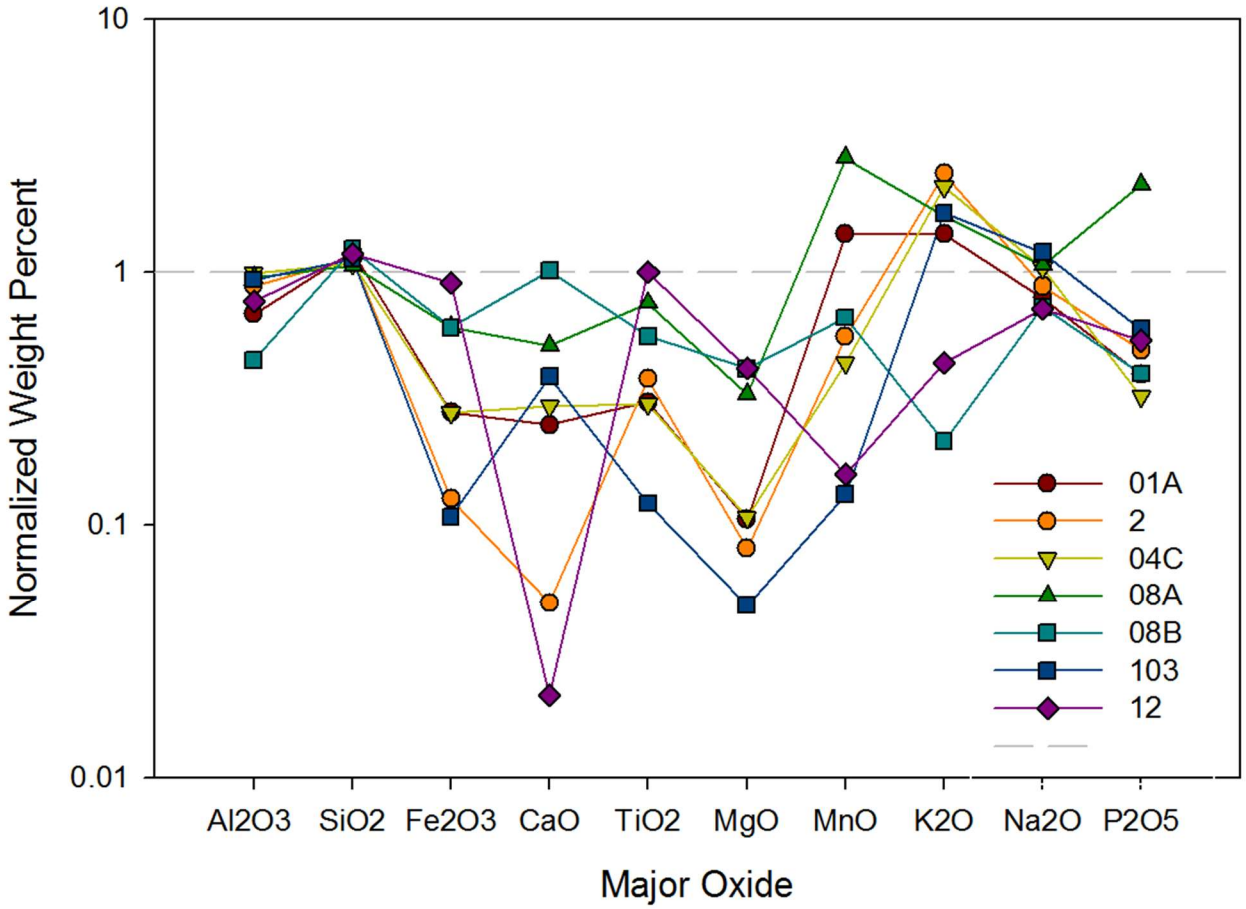

Figure 6: Major oxide percents of seven samples normalized to upper continental crust major oxide composition (Rudnick and Gao, 2003). The x-axis uses a logarithmic scale with 1 being the composition of upper continental crust.

Mineralogy

Both light microscopy and scanning electron microscopy show an abundance of quartz, albite, and epidote throughout all samples. Albite were observed in every sample and epidote in the all samples except for 08B. Mineral grains such as epidote, garnet, apatite, and rare earth bearing mineral phases show evidence of alteration across a range of samples. In Sample 12, epidote grains surrounded by albite showed chemical differences between the outer rim and the interior of grains (Figure 7).

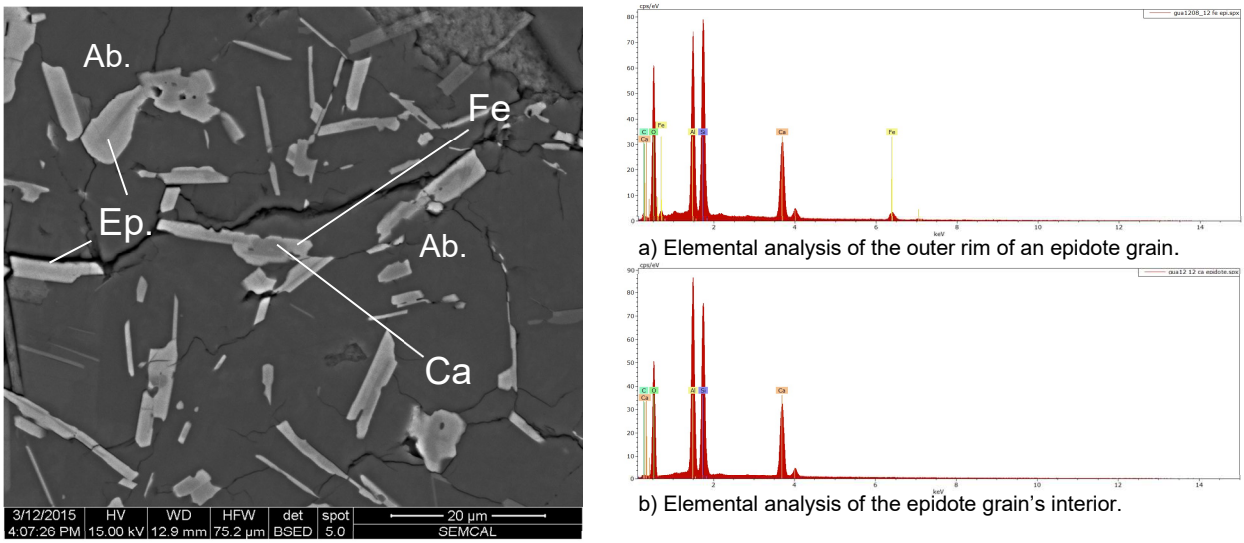

a) Elemental analysis of the outer rim of an epidote grain.

b) Elemental analysis of the epidote grain's interior.

Figure 7: Epidote grains in a groundmass of albite show different compositions within single grains.

In sample 08B, which has a similar CaO concentration as upper continental crust, carbonate with iron and magnesium was found throughout the rock (Figure 8). Iron oxy hydroxides coincide with the Fe-Mg rich carbonate. Moving from the interior to the exterior of Sample 08B the amount of pore space increases as the amount of carbonate decreases (Figure 9). Elemental mapping images show the presence of Ca, Al, and Fe in the outer rim of the sample (Figure 9). The aluminum is representative of the albite in the sample and the iron shows how the iron oxides frame the calcium and Fe-Mg rich calcium carbonate.

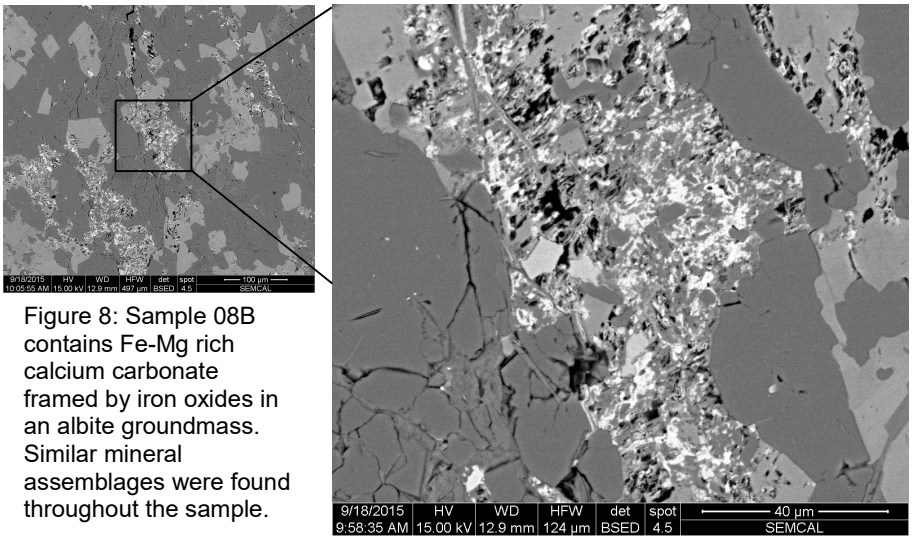

Figure 8: Sample 08B contains Fe-Mg rich calcium carbonate framed by iron oxides in an albite groundmass. Similar mineral assemblages were found throughout the sample.

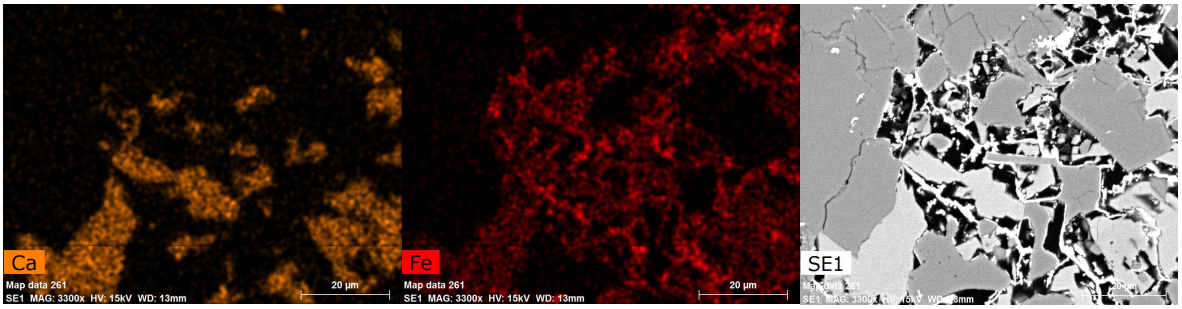

Figure 9: Elemental mapping of the outer rim of sample 08B which shows more pore spaces than the interior of the rock. The calcium map shows the location of carbonate. The iron map shows how iron has infiltrated the carbonate and how iron oxy hydroxides frame the dissolved carbonate.

Dissolution textures on euhedral garnet crytals were observed across a range of samples (Figure 10). These garnets were observed on broken pieces of cobbles, rather than in thin section, from both the interior and exterior of the rocks. The garnet in these samples was found in a groundmass of quartz, albite, and weathered clay minerals. In some cases euhedral grains also appeared to be fractured in addition to the etched mineral surface.

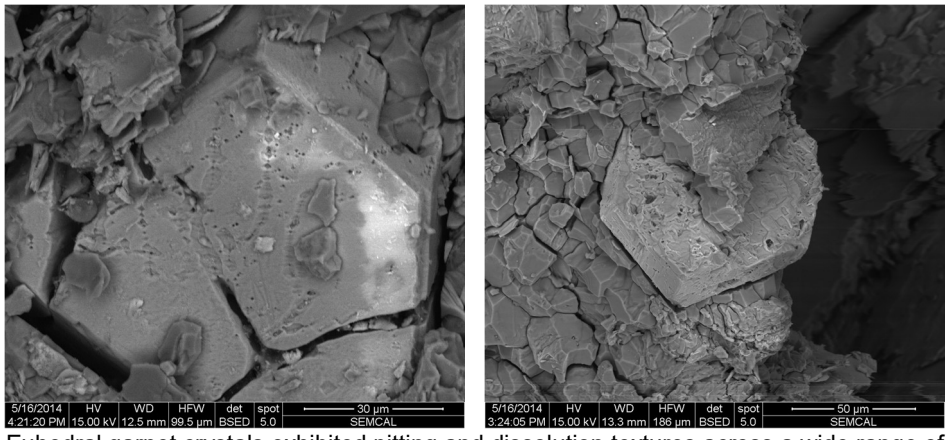

Figure 10: Euhedral garnet crystals exhibited pitting and dissolution textures across a wide range of samples. Crystals were found in a groundmass of albite and quartz.

Apatite, another major mineral constituent of the rock samples was found to have extensive weathering across a range of rock types. Dissolution textures, mineral precipitates and biogenic remains appeared on the broken surface of apatite crystals (Figure 11).

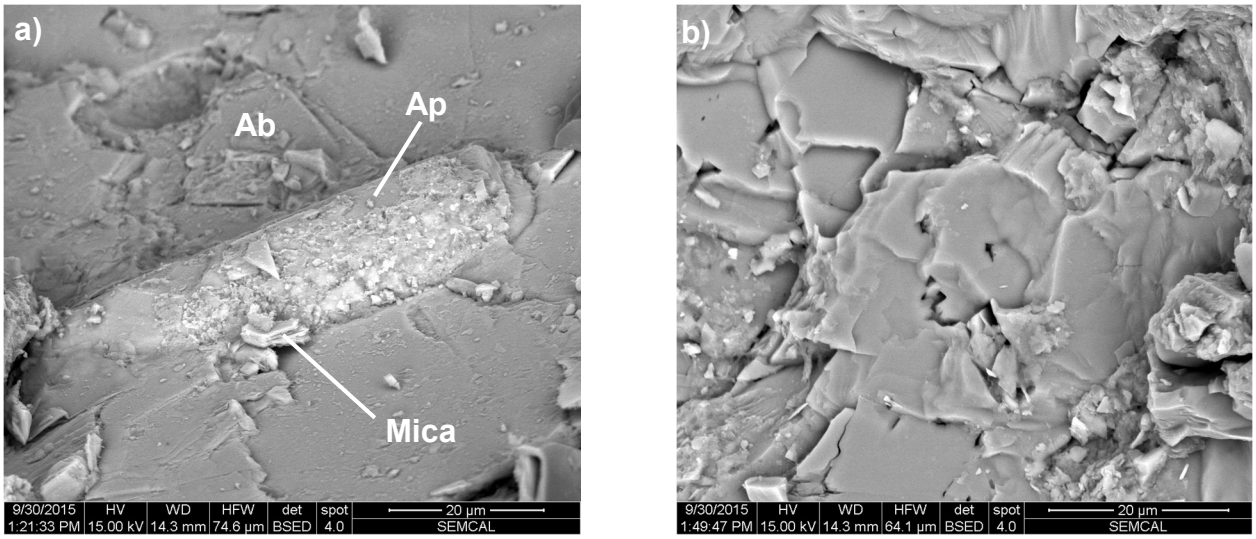

Figure 11: a) Apatite grain in a groundmass of albite and mica. The apatite grain is covered in mineral precipitates and remnant biofilm. b) Broken apatite surface with dissolution pits. Clay minerals and mineral precipitates are also seen on this sample.

Clays surround by relatively unweathered micas and albite were observed in sample 08A (Figure 12). Micas next to the clay show weathering along one side of the grain but not on the other side. Due to the extensive weathering of the clays a reliable elemental spot analysis was not attainable.

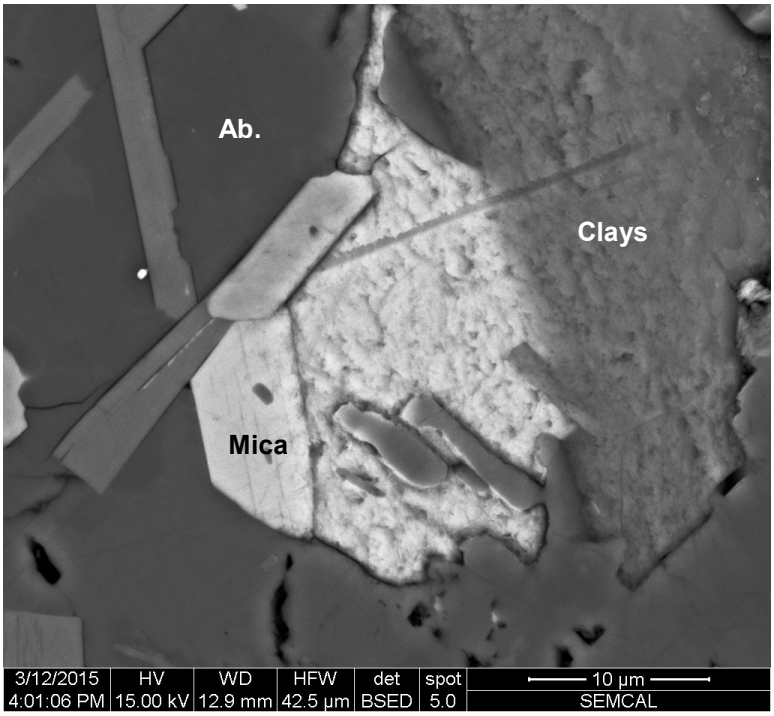

Figure 12: Weathered clay minerals surround by relatively unweathered micas and albite in sample 08A.

Rare Earth Bearing Mineral Phases

Rocks samples also included an abundance of rare earth bearing mineral phases. These minerals included monazite, allanite (REE bearing epidote) and xenotime. Monazites enriched in thorium and a variety of REE like Ce and La show extensive weathering on the mineral surface and exhibited a fluffy, flaky texture. Allanite exhibits a different texture. Allanite grains contained extensive etch pits that gave the mineral surface a “sponge-like” texture (Figure 13). Spot analysis of these allanite grains show the presence of REEs such as, Ce, La and Nd. Xenotime, a yttrium orthophosphate, was observed in a high-grade metamorphic sample that also contained relatively high quantities of graphite.

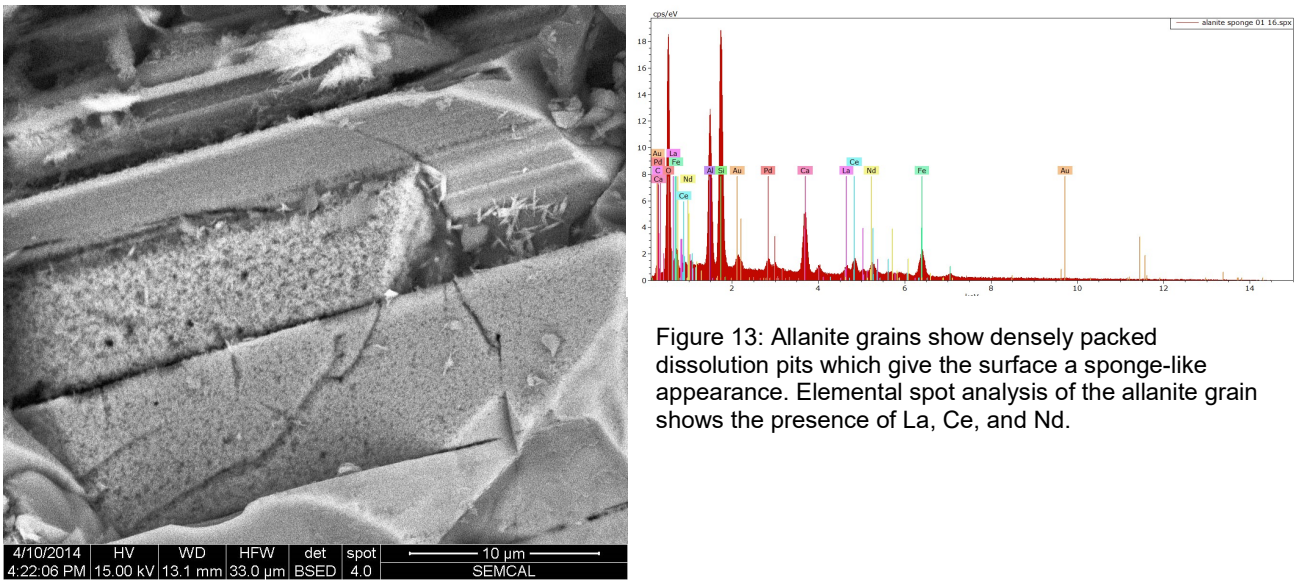

Figure 13: Allanite grains show densely packed dissolution pits which give the surface a sponge-like appearance. Elemental spot analysis of the allanite grain shows the presence of La, Ce, and Nd.

Discussion

Weathering of the Rock Interior

The original goal of this study was to use the interior of the rock samples as a proxy for the unweathered origin of the weathered exterior of the rocks. Upon investigation it was found that the interior of the rocks had been subject to weathering via fractures. Every rock sample observed using the SEM showed signs of chemical weathering in the interior. In sample 08A, mica was seen to be weathered on only one side which is suggestive of secondary clay formation due to chemical weathering.

Origins of Minerals

Previous studies have shown that lithology is a significant control on carbonate weathering. It was also observed by McAdams that bicarbonate is the most commonly seen anion in the stream chemistry in all samples collected in La Sierra de las Minas (McAdams et al., 2015). Brocard et al. (2011) linked the bicarbonate in the water chemistry to the Chóchal Formation and the Santa Rosa group (which consists of fossiliferous shales) but carbonate was observed only in one stream cobble examined herein (Brocard et al., 2011). The carbonate weathering may not be controlled solely by physical weathering, but also by chemical influences such as hydrothermal alteration, dissolution, or ferrolysis.

Calcium Contributors

Mineralogy is a leading control of the calcium input into small mountainous river systems (Jacobson and Blum, 2003). In the present study, minerals such as albite, allanite, carbonates, garnet, and apatite are all possible contributors to the calcium concentration found in the stream chemistry. The bedrock of La Sierra de las Minas includes both gypsum and limestone units, and in particular, the Chixóy River is underlain by a gypsum unit (Brocard et al., 2011).

Due to its stoichiometry, albite's weathering may not be the largest calcium contributor to stream aqueous chemistry, but albite is seen across all samples in some quantity. In small quantities albite's contribution of calcium to stream geochemistry is negligible, but when as seen here, in large quantities in a range of samples albite should be taken into account when predicting the calcium flux. Seen in smaller quantities, but still important were garnet and apatite. Both minerals exhibited dissolution textures in multiple samples. In the most extreme of cases, in the presence of iron oxyhydroxides, carbonate appeared to be completely dissolved, as indicated by increasing pore space towards the exterior of the rock (Figure 8). The same is possible for allanite, which is discussed in the following section.

Implications of Epidote-Group Weathering

The phrase "calcium problem," first introduced by Bowser and Jones (2002), is used to describe the higher Ca/Na ratios in streams than anticipated from the dissolution of potassium feldspar. While epidote has been thought to be resistant to weathering, similar to quartz and zircon, numerous studies have shown the opposite for the REE bearing phase of epidote, allanite (Price et al., 2005).

Research conducted by Price et al. (2005) in the U.S. Forest Service Coweeta Hydrologic Laboratory showed allanite to be highly weatherable and epidote to be resistant to weathering. SEM analysis of samples from la Sierra de las Minas shows similar results. Epidote grains, which have elemental differences within individual grains (Figure 7), do not show the extensive etch pits that allanite grains exhibit (Figure 12). While allanite is not a major mineral constituent observed in the stream cobbles, its easily weathered nature makes it a likely source of calcium.

In addition to providing calcium, allanite is also responsible for the dissolution products such as REEs and iron. The A2 sites of allanite have the ability to contain REE ions, such as Ce and Sr, as well as Pb, rather than calcium. REEs are mobile during weathering, with the exception of Ce, which has the ability to oxidize and precipitate as cerianite (CeO_2). Although, monazite has been shown to fix these REEs before being transported a notable distance, this cannot be confirmed with currently available data. In addition to Ce, Fe oxidizes more readily in allanite than in epidote due to the higher energy of the sites containing Fe (Price et al., 2005).

Ferrolysis and Carbonate Dissolution

Iron oxyhydroxides were found in a sample that contained carbonates and shows evidence of carbonate dissolution (Figure 9). One likely cause of this dissolved carbonate was the incorporation of iron within and around the carbonate. $FeCO_3$, siderite, has a pKa of -10.7 which is less soluble than $CaCO_3$ with a pKa of -8.35 (Smith, 1976), therefore the incorporation of iron into the carbonate was unlikely to have caused the carbonate to dissolve. Rather, the presence of iron caused ferrolysis to take place. Ferrolysis is the hydrolysis of iron which in turn forms an acid. The process also makes metals such as iron and aluminum more soluble in water. (Mann, 1983).

Conclusions

The analyses of stream cobble samples showed mineralogy and major oxide concentrations that are consistent with the water analyses. Minerals such as epidote, albite, apatite, garnet, Fe-Mg rich calcite and allanite are very likely to have contributed to the flux of calcium in the water. This is supported by their dissolution textures and fractures exhibited under SEM.

Overall, the UCC-normalized major oxide analysis supports a high extent of rock weathering. The majority of samples show depletions of all major oxides, with the exception of one or more samples being enriched in Mn, K, and P. Further investigation is required to determine the causes of these enrichments. All samples showed a depletion in calcium with the exception of sample 08B, which contains significant quantities of calcium carbonate. Not all samples fall into the bulk composition of upper continental crust, like sample 08B. Thus the use of the upper continental crust as the proxy for unweathered stream cobbles has its drawbacks and may not be the best choice for normalization.

SEM images showed extensive weathering of accessory minerals such as monazite, xenotime and ilmenite. While these minerals appear in small quantities within their respective rocks, when taken into account at a larger scale it is possible for these minerals to have a quantitative impact on solute production, especially Ca^{2+} in these waters.

RECOMMENDATIONS FOR FUTURE WORK

This study focused on the north side of La Sierra de las Minas. Analysis of the south side of the mountain range, which receives noticeably less precipitation, has the possibility to provide evidence on the significance of precipitation on calcium weathering in small mountainous river systems.

When normalized to major oxide concentrations of upper continental crust, some samples appeared to be enriched in Mn, K and P. Further investigation is needed in order to determine the cause of this enrichment such as looking at samples under the SEM with the purpose of finding minerals rich in Mn, K and P. It would also be advantageous to compare each rock individually to a better suited unweathered proxy based on the mineralogy of each sample. This would provide a more accurate conclusion as to which samples were depleted in particular elements and therefore their contribution to the weathering flux.

Among microcopy and XRF results, x-ray diffraction analysis was performed on 7 samples, two of which have not been viewed under a microscope. XRD data would solidify the mineralogy determined from light and scanning electron microscopy. It would also provide quantified data of the mineralogy of stream cobbles.

REE bearing trace minerals were also seen in all samples in this study. While major ions have been evaluated, analysis of REE has not been performed in the stream water samples. Determination of the presence of the REE elements in the streams would help to determine the mobility of REE as they are chemically weathered from minerals such as allanite, monazite and xenotime. Furthermore, these additional data would create a more robust chemical analysis of the water samples and could lead to investigation of other minerals responsible for the high chemical weathering rates of La Sierra de las Minas.

REFERENCES CITED

Bowser, C.J., Jones, B.F., 2002. Mineralogic controls on the composition of natural waters dominated by silicate hydrolysis. Am. J. Sci. doi:10.2475/ajs.302.7.582

Brocard, G., Teyssier, C., Dunlap, W.J., Authemayou, C., Simon-Labric, T., Cacao-Chiquín, E.N., Gutiérrez-Orrego, A., Morán-Ical, S., 2011. Reorganization of a deeply incised drainage: Role of deformation, sedimentation and groundwater flow. Basin Res. 23, 631–651. doi:10.1111/j.1365-2117.2011.00510.x

Bundschuh, J., 2007. Central America : geology, resources and hazards. Taylor & Francis, London ;;New York.

Carey, A.E., 2005. Organic carbon yields from small, mountainous rivers, New Zealand. Geophys. Res. Lett. 32, L15404. doi:10.1029/2005GL023159

Goldsmith , S.T., 2005. Geochemical fluxes and weathering on high standing islands : Taranaki and Manawatu-Wanganui regions New Zealand (Thesis). URL http://rave.ohiolink.edu/etdc/view?acc_num=osu1391601668

Goldsmith, S.T., Moyer, R.P., Harmon, R.J., 2015. Hydrochemistry and biogeochemistry of tropical small mountain rivers. Appl. Geochemistry 63, 453–455. doi:http://dx.doi.org/10.1016/j.apgeochem.2015.11.005

Jacobson, A.D., Blum, J.D., 2003. Relationship between mechanical erosion and atmospheric CO2 consumption in the New Zealand Southern Alps. Geology 31, 865. doi:10.1130/G19662.1

Lyons, W.B., 2005. Chemical weathering in high-sediment-yielding watersheds, New Zealand. J. Geophys. Res. 110, F01008. doi:10.1029/2003JF000088

Mann, A.W., 1983. Hydrogeochemistry and weathering on the Yilgarn Block, Western Australia-ferrolysis and heavy metals in continental brines. Geochim. Cosmochim. Acta 47, 181–190. doi:10.1016/0016-7037(83)90131-X

Marshall, J.S., 2007. Chapter 3 The Geomorphology and Physiographic Provinces of Central America. Cent. Am. Geol. Resour. Hazards-Bundschuh Alvarado 1 1–51. doi:n/a

McAdams , B.C., 2012. Chemical weathering and organic carbon transport in an active mountain belt : Sierra De Las Minas, Guatemala (Thesis). URL http://rave.ohiolink.edu/etdc/view?acc_num=osu1354722072

McAdams, B.C., Trierweiler, A.M., Welch, S.A., Restrepo, C., Carey, A.E., 2015. Two sides to every range: Orographic influences on CO2 consumption by silicate weathering. Appl. Geochemistry 63, 472–483. doi:10.1016/j.apgeochem.2015.04.010

Milliman, J.D., Syvitski, J.P.M., 1992. Geomorphic/Tectonic Control of Sediment Discharge to the Ocean: The Importance of Small Mountainous Rivers. J. Geol. doi:10.1086/629606

Price, J.R., Velbel, M.A., Patino, L.C., 2005. Allanite and epidote weathering at the Coweeta Hydrologic Laboratory, western North Carolina, U.S.A. Am. Mineral. doi:10.2138/am.2005.1444

Rudnick, R.L., Gao, S., 2003. Treatise on Geochemistry, Treatise on Geochemistry. Elsevier. doi:10.1016/B0-08-043751-6/03016-4

Smith, R., 1976. Critical stability constants.

APPENDIX

Appendix A

Glass bead making method is modified from Goldsmith (2005).

1. Samples were broken into pieces less than 5mm in any direction using a rock hammer. An equal amount of weathered exterior rock and the interior of the rock was used.
2. Roughly 10 grams of broken sample was placed into a SPEX CentriPrep 8515 Shatterbox and crushed for a minimum of 60 seconds for a competent rock (such as granite, gneiss, heavily compacted rocks).
3. The powder was then transferred to a porcelain crucible to be dried for a minimum of 12 hours at 110°.
4. After drying, 2.5 grams of the powdered rock sample was mixed with 10 grams of lithium tetraborate flux. This is a 1:4, sample to flux ratio.
5. The sample and flux mixture was then transferred to platinum crucible and placed in a Philips Perl'x 3 and heated to roughly 1220°C.
6. The liquid is then cast into a platinum dish to form a glass bead.
7. Once cooled, each bead was labeled and stored in a plastic dish in a desiccator until ready for XRF analysis.

Appendix B

Summary of Major Oxide Concentrations Corrected to 100%

Sample	Al_2O_3 (wt. %)	SiO_2 (wt. %)	Fe_2O_3 (wt. %)	CaO (wt. %)	TiO_2 (wt. %)	MgO (wt. %)	MnO (wt. %)	K_2O (wt. %)	Na_2O (wt. %)	P_2O_5 (wt. %)
01A	14.53	73.32	1.41	1.02	0.52	0.29	0.17	5.52	3.16	0.06
2	13.54	75.36	0.64	0.18	0.24	0.20	0.06	6.85	2.87	0.07
04C	15.23	72.29	1.40	1.06	0.19	0.26	0.04	6.07	3.41	0.05
08A	14.60	70.48	3.04	1.83	0.48	0.82	0.28	4.66	3.48	0.33
08B	6.93	81.91	3.04	3.64	0.36	1.03	0.07	0.60	2.37	0.06
103	14.36	74.73	0.54	1.39	0.08	0.12	0.01	4.78	3.91	0.09
123	11.75	78.28	4.55	0.08	0.64	1.03	0.02	1.23	2.34	0.08

Appendix C

XRD analysis raw data.

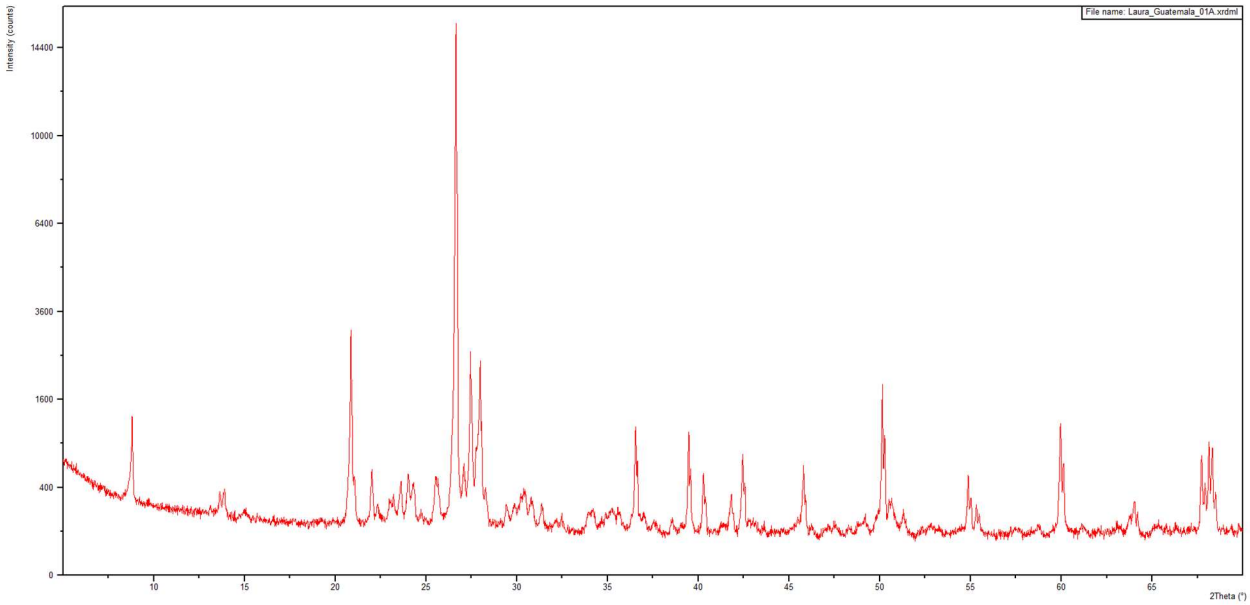

Sample 01A

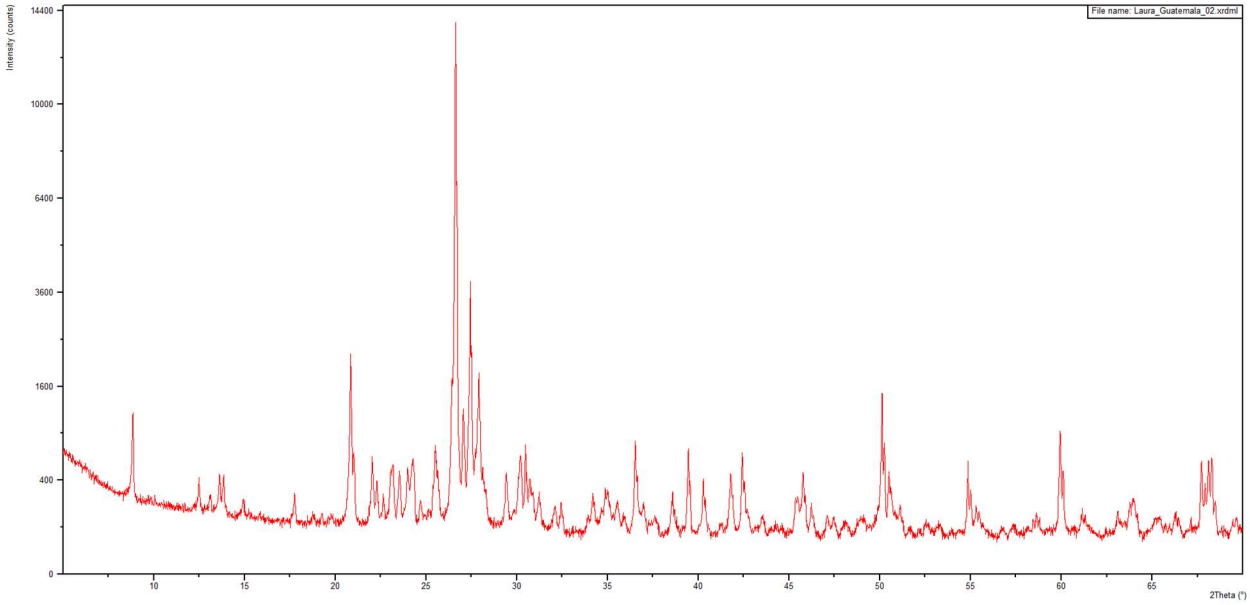

Sample 02

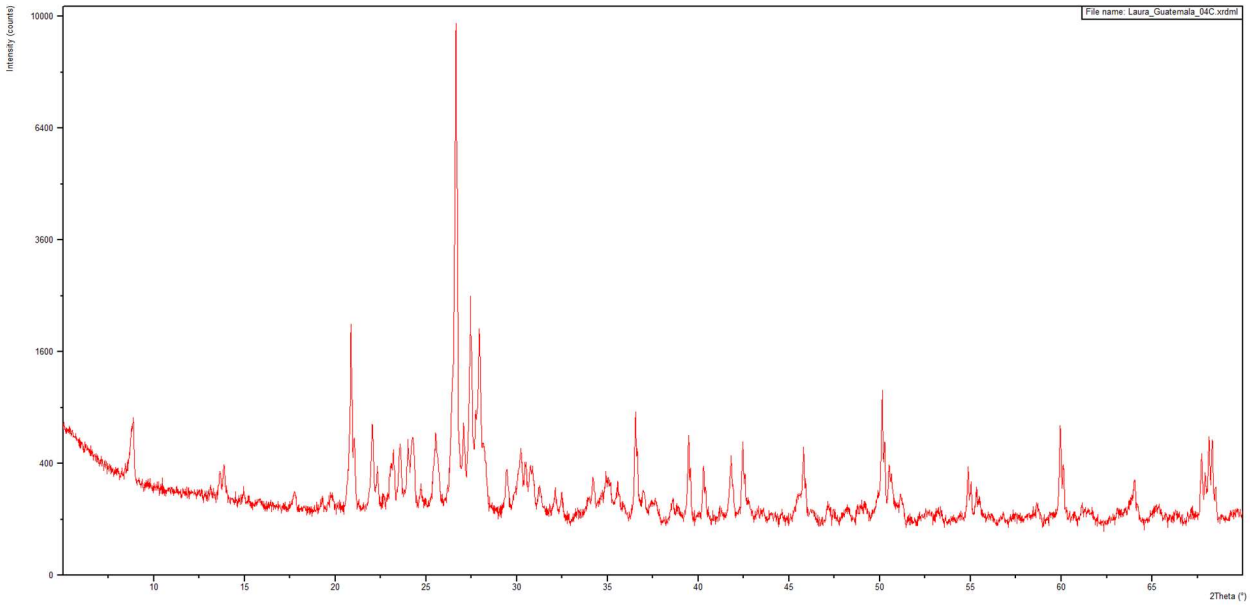

Sample 04C

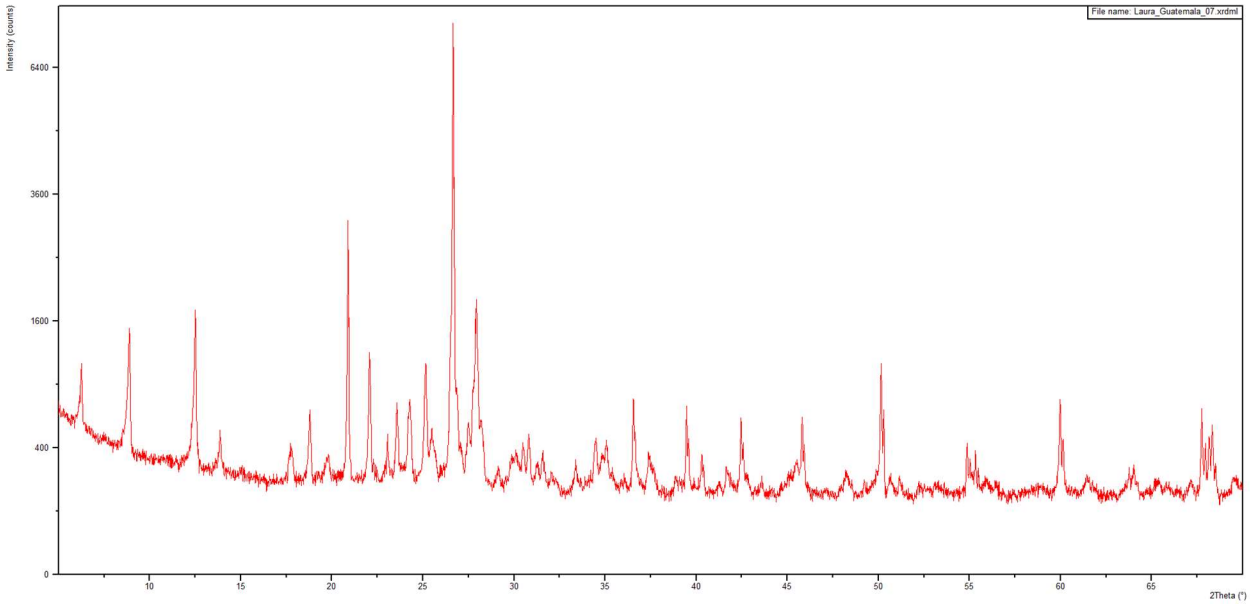

Sample 07

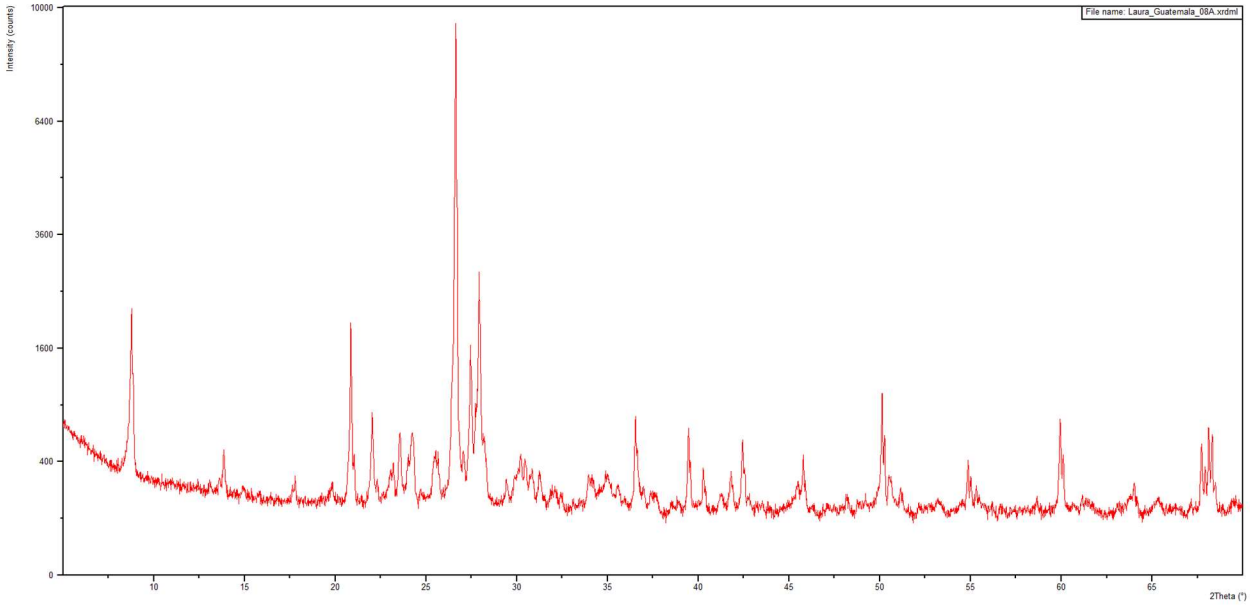

Sample 08A

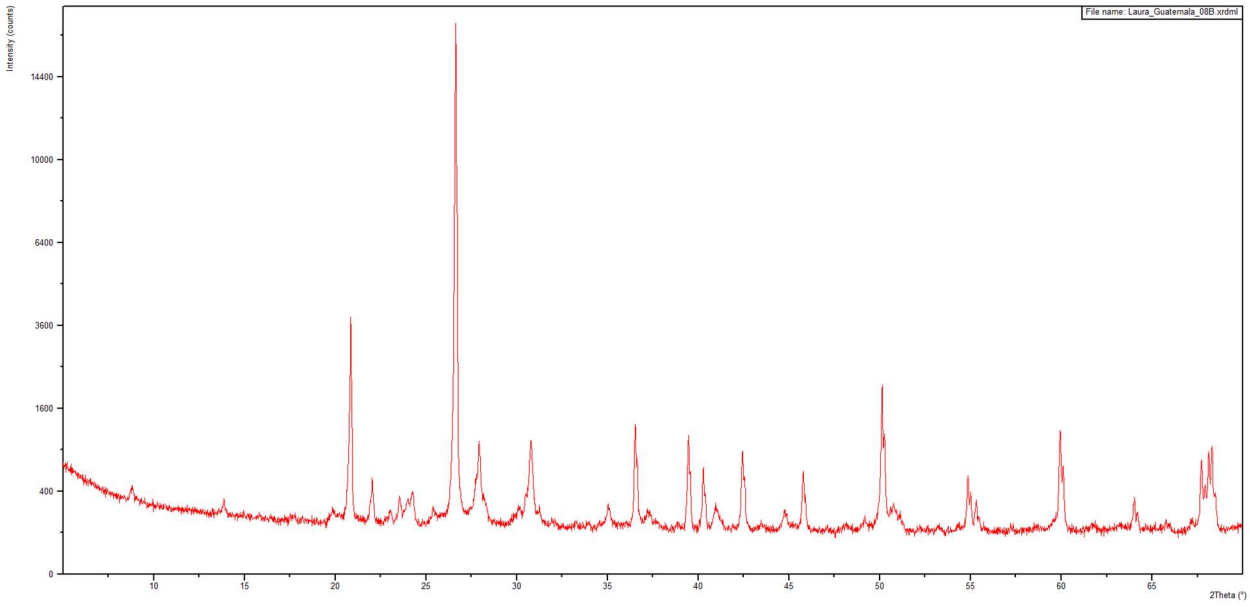

Sample 08B

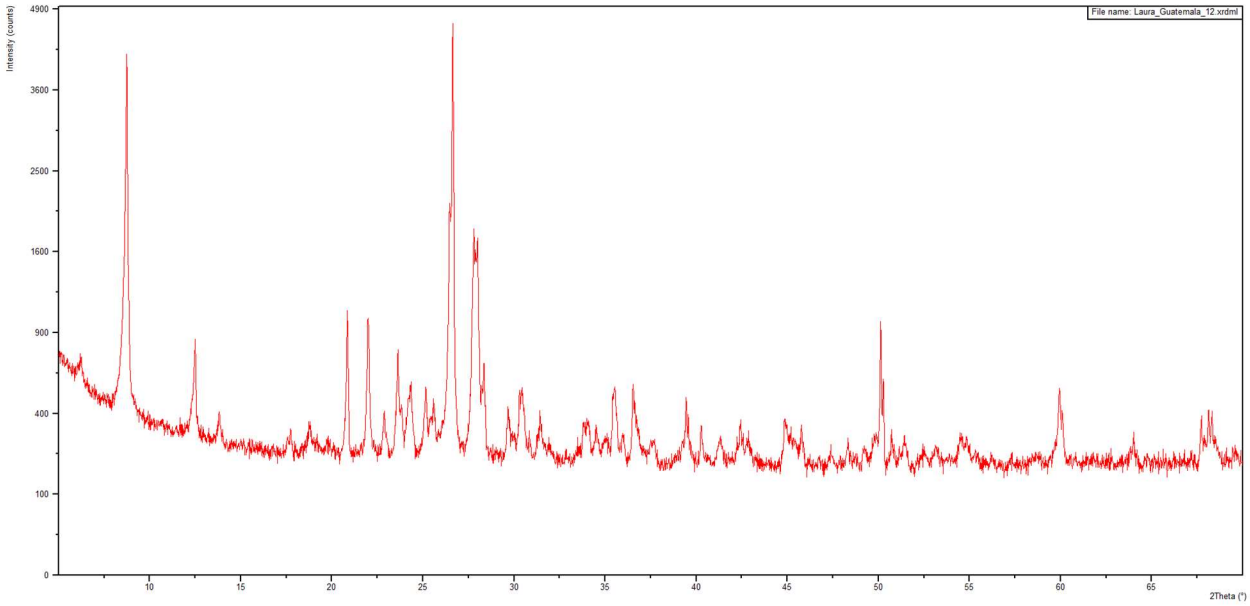
File name: Laura_Guatemala_12.xrdml
Intensity (counts)
4900
3600
2500
1600
900
400
100
0
10
15
20
25
30
35
40
45
50
55
60
65
2Theta (°)

Sample 12